Final Technical Report
November 2011

MEMBRANE PURIFICATION CELL
FOR
ALUMINUM RECYCLING

Final Technical Report

Membrane Purification Cell for Aluminum Recycling

DOE Award Number: DE-EE0003466

Project Period: August 16, 2010 – August 15, 2011

Authors: David H. DeYoung, 724-337-2269,
david.deyoung@alcoa.com
Cong Wang, 724-337-2112,
cong.wang@alcoa.com
James Wiswall, 724-337-4529,
james.wiswall@alcoa.com

Business Contact: Sara Yount, 724-337-3256,
sara.yount@alcoa.com

Alcoa Inc.
Alcoa Technical Center
100 Technical Dr.
Alcoa Center, PA 15069-0001

November 28, 2011

Acknowledgment: This report is based upon work supported by the U. S. Department of Energy under Award No. DE-EE0003466.

Contents

Tables

Figures

List of Symbols and Acronyms

Symbol	Description
A	anode surface area
AW_{Al}	atomic weight of aluminum
c_e	cost of electricity per mass ($/lb)
C_e	cost of electricity ($/kWh)

c_s	cost of scrap
E	energy per mass requirement
ε_j	current efficiency
F	Faraday's constant
l	anode to cathode distance
j	current density
m	Mass
$\dot{m}$	mass flow rate
M	molecular weight
n	number of electrons transferred per aluminum atom
ρ	Resistivity
P	electric power
r_p	purified recovery
t	Time
v	value per mass purified
V	Voltage
v_d	value of the downgrade
v_p	value of the purified product
z	valence number of ions

ACD	anode-cathode distance
ARV	anode reference voltage
CRV	cathode reference voltage
BSE	back-scattered electron
EDS	energy dispersive spectrum
EBITDA	earnings before interest, taxes, depreciation, and amortization
ICP	inductively coupled plasma
LME	London metal exchange
SEM	scanning electron microscopy
UBC	used beverage cans

1.0 Executive Summary

Recycling aluminum scrap currently requires adding an average of 33% primary aluminum to the scrap stream to offset contamination with non-aluminum alloy constituents and to handle mixed-alloy scrap streams. Adding primary aluminum significantly increases the energy required for recycling, because primary aluminum production requires approximately 10 times more energy than melting scrap. Eliminating the need for using primary aluminum as a diluent would enable several viable commercial applications, such as producing pure aluminum diluent from purchased scrap; recycling brazing sheet, consumer packaging, and multi-alloy, laminated products; recovering Al from mixed alloy saw chips and lithium from Al-Li mixed scrap.

This project was aimed at developing an electrorefining process for purifying aluminum to reduce energy consumption and emissions by 75% compared to conventional technology. An electrolytic molten aluminum purification process, utilizing a horizontal membrane cell anode, was designed, constructed, operated and validated. The electrorefining technology could also be used to produce ultra-high purity aluminum for advanced materials applications.

The technical objectives for this project were to:

- Validate the membrane cell concept with a lab-scale electrorefining cell;
- Determine if previously identified voltage increase issue for chloride electrolytes holds for a fluoride-based electrolyte system;
- Assess the probability that voltage change issues can be solved; and
- Conduct a market and economic analysis to assess commercial feasibility.

The process was tested using three different binary alloy compositions (Al-2.0 wt.% Cu, Al-4.7 wt.% Si, Al-0.6 wt.% Fe) and a brazing sheet scrap composition (Al-2.8 wt.% Si-0.7 wt.% Fe-0.8 wt.% Mn). Purification factors (defined as the initial impurity concentration divided by the final impurity concentration) of greater than 20 were achieved for silicon, iron, copper, and manganese. Cell performance was measured using its current and voltage characteristics and composition analysis of the anode, cathode, and electrolytes. The various cells were autopsied as part of the study.

Three electrolyte systems tested were: LiCl-10 wt.% $AlCl_3$, LiCl-10 wt.% $AlCl_3$-5 wt.% AlF_3 and LiF-10 wt.% AlF_3. An extended four-day run with the LiCl-10 wt.% $AlCl_3$-5 wt.% AlF_3 electrolyte system was stable for the entire duration of the experiment, running at energy requirements about one third of the Hoopes and the conventional Hall-Heroult process.

Three different anode membranes were investigated with respect to their purification performance and survivability: a woven graphite cloth with 0.05 cm nominal thickness & > 90 % porosity, a drilled rigid membrane with nominal porosity of 33%, and another drilled rigid graphite membrane with increased thickness. The latter rigid drilled graphite was selected as the most promising membrane design.

The economic viability of the membrane cell to purify scrap is sensitive to primary & scrap aluminum prices, and the cost of electricity. In particular, it is sensitive to the differential between scrap and primary aluminum price, which is highly variable and dependent on the scrap source. In order to be economically viable, any scrap post-processing technology in the U.S. market must have a total operating cost well below the scrap price differential of $0.20-$0.40 per lb to the London Metal Exchange (LME), a margin of 65%-85% of the LME price. The cost to operate the membrane cell is estimated to be < $0.24/lb of purified. The energy cost is

estimated to be $0.05/lb of purified with the remaining costs being repair and maintenance, electrolyte, labor, taxes, and depreciation.

The bench-scale work on membrane purification cell process has demonstrated technological advantages and substantial energy and investment savings against other electrolytic processes. However, in order to realize commercial reality, the following items need to be fully investigated:

1. Further evaluation of a pure fluoride electrolyte.
2. Investigate alternative non conductive, more mechanically robust and chemically inert membrane candidates.
3. Optimized membrane cell design to understand contribution of fluid flow patterns and the mass transfer conditions.
4. Close the loop on the system mass balance.

All Tasks and Milestones were completed successfully.

2.0 Introduction/Background

The concept of electro-refining aluminum via molten salt electrolysis was first demonstrated in the Hoopes three-layer process in the 1920s [1]. In this method, the impure aluminum anode forms the dense bottom layer, a suitable electrolyte of lower density is placed as the middle layer, and the purified metal cathode forms on top of the electrolyte layer. Electrolyte compositions are selected to have a density intermediate between the pure metal and the alloyed impure metal so as to obtain good separation between the three layers (often contains $BaCl_2$ and BaF_2). A current is then passed from the positively charged impure metal layer to the negatively charged pure metal layer. Aluminum ions are transported across the salt layer according to Faraday's Law of Electrolysis:

$$m = \frac{ItM}{Fz}$$

Where the m is the mass of Al transferred, I is the current (amps), M the molecular weight of Al (g/mole), F is Faraday's constant, t is time (s), and z is the valence number of ions transferred.

The process is still commercially operated in several countries (Norway, Germany, Russia and China) for the refining of potroom metal to 99.99% purity or better. The theoretical energy requirements of the process are low since only a very low voltage difference of approximately 0.1V is needed to transfer Al ions from an activity of ~ 0.7 in the anode to unit activity in the cathode. In practice, however, the Hoopes cells operate at ~ 5 V and the energy requirements are ~ 15 kWh/kg, which is comparable to the conventional Hall-Heroult process for the electrolysis of alumina to produce aluminum. The main reason for this is the need to have a thick electrolyte layer (6 – 10 inches) to prevent direct mixing between the impure and pure metal layers due to fluid motion caused by electromagnetic and thermal forces. This results in high resistive losses. The thick electrolyte layer and the low conductivity of suitable electrolytes limits the extensive application of the Hoopes cell as a scrap purification process.

An electro-refining process was developed by Alcoa in the 1970s that utilized a membrane, composed of either porous carbon or graphite cloth, to separate the anodic and cathodic metal layers. By mechanically separating the anode and cathode, the anode-cathode distance could be greatly reduced as compared to the Hoopes cell and high resistive losses would be reduced. Additionally, the electrolyte was switched to less-dense chloride salt, such as LiCl-10 wt.% $AlCl_3$, which has a relatively low melting temperature and is highly conductive [2].

Although significant development of the membrane cell to purify molten aluminum was pursued by Alcoa in the late 1970s to early 1980s [3, 4, 5], the effort was ultimately terminated because of a technical problem – a gradual increase in cell voltage which contributed to higher than expected energy consumption. Also, the relatively low price of primary aluminum at the time resulted in a diminished business case. The business case for the purification technology now appears far more attractive in light of current energy and environmental factors.

The current project focused on verifying previous work and solving the voltage increase issue. The overall approach was to construct a bench-scale cell and use it to conduct tests to validate the expected purification factors on several scrap types. The membrane cell was then tested for durability using different electrolyte systems with selected membrane candidates to screen for potential issues. Special attention was given to the problem previously identified but not solved—gradual voltage increases leading to high over-potential on the anode surface, which

happened concurrently with $AlCl_3$ depletion over time during continuous operation. The hypothesis postulated was that this degradation was due to gradual build up of oxides in a chloride bath, and could be avoided by utilizing a fluoride bath.

The Alcoa-DOE *Membrane Purification Cell for Aluminum Recycling* project was divided into six Tasks with three major Milestones:

Tasks

1. Laboratory-Scale Concept Validation of Purification
2. Cell Voltage Characteristics
3. Cell Autopsies
4. Economic Modeling and Market Assessment
5. Potential Benefits Assessment
6. Project Management and Reporting

Milestones:

I. Successful operation of the Membrane Cell for upgrading scrap with silicon, iron and copper purification factors greater than 20.

II. Completion of cell autopsy to understand the root cause for voltage increases.

III. Delivery of Final Report to include technical and economic assessment, energy and environmental benefits with recommendations.

A schematic of the membrane purification cell is presented in Figure 1. The cell is composed of an inner graphite cylinder containing the aluminum scrap and an outer graphite cylinder containing the electrolyte. The graphite cloth membrane is attached to the bottom of the inner cylinder. The inner cylinder is attached to the positive end of a power source and becomes the anode. The outer cylinder is connected to the negative end and acts as the cathode. Figure 1 illustrates the horizontal arrangement of the membrane used in the present study. It allows the anode-cathode distance to be easily adjusted during an experiment. This design is a deviation from that used in the earlier work in which the membrane anode was cemented on the vertical wall of the inner cylinder, which limited the ability to adjust anode-cathode distances.

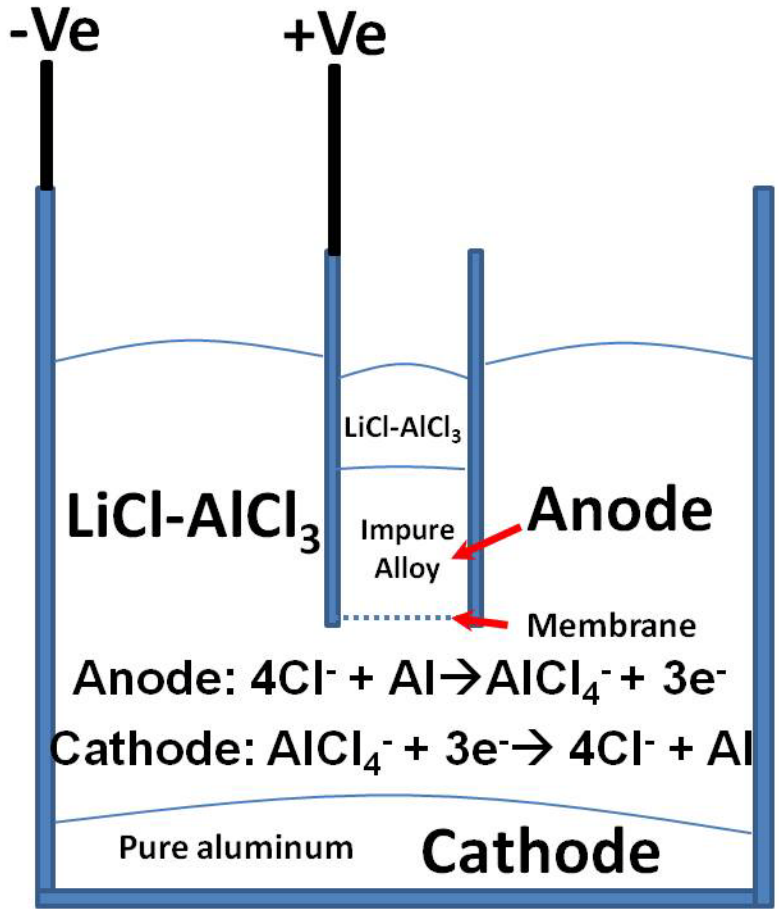

Figure 1 - Schematic of the membrane cell electrolytic purification process.

Once everything is molten and the electrical connections are established, the anodic and cathodic reactions can be initiated. Aluminum from the scrap alloy becomes ionized at the electrolyte-alloy interface according to the following reaction:

$$4Cl^- + Al = AlCl_4^- + 3e^-$$

$AlCl_4^-$ ions permeate the membrane and diffuse through the electrolyte to the cathode, where $AlCl_4^-$ will be reduced to pure aluminum via the opposite reaction:

$$AlCl_4^- + 3e^- = 4Cl^- + Al$$

In this way, purified aluminum accumulates in the cathode while the noble (less electro-negative) impurities (such as Fe and Si) contained in the scrap are enriched in the anode.

3.0 Results and Discussion

3.1 Bench scale cell design

The current work's bench-scale cell follows Martchek's [4] "mini-cell" design, broken down into the following four major parts: (See Figure 2)

a. The graphite anode cylinder has an inner diameter of 2.0 in and a height of 4.0 in. to accommodate the impure alloy. The anode cylinder is shrouded by an insulating alumina liner (shown in pink) except for the region of the membrane assembly to assure that the current flows through the membrane.
b. The cathode is also made of graphite. An alumina liner is positioned inside the graphite cathode (shown in pink) to electrically insulate the sidewalls and assure current flow downward to the cathode bottom. In between the cathode and the anode, electrolyte will be charged to serve as the conductive medium.
c. The membrane is installed on the bottom of the anode cavity.
d. The inconel outer shell serves as an electrical ground and provides containment of the cell components (shown in black).

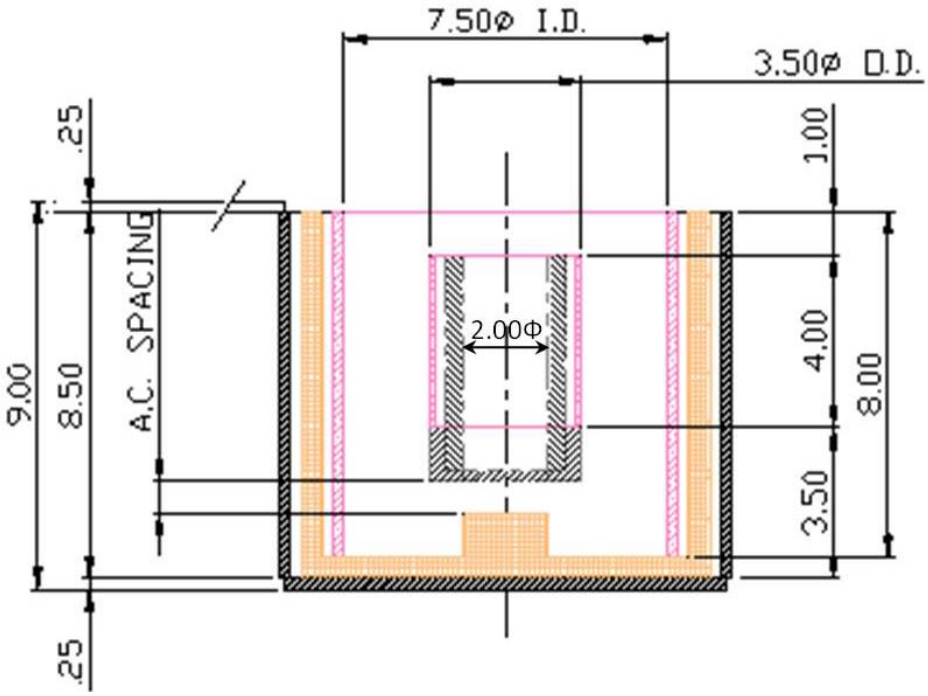

Figure 2 - Schematic illustration of the cell design

A power supply with voltage ranging from 0 to 10 v and current from 0 to 200 A was employed for the bench-scale tests.

Anode, cathode, membrane, liner, and outer shell materials of construction used in this design are listed in Table 1.

Table 1 - Material Specification for Major Components

Material	Composition	Remarks
Anode	ATJ graphite[1]	Electrode grade
Cathode	ATJ graphite	Electrode grade
Membrane	Graphite cloth	0.05 mm nominal thickness, +90% porosity
	Drilled rigid graphite	0.8 mm hole diameter, 0.8 mm and 3.0 mm thicknesses, 33% porosity
Liner	99.95% pure alumina	--
Inner wall	ATJ graphite	Electrode grade
Outer shell	Inconel	Grounding point

3.2 Characterization techniques

- X-ray diffraction (XRD) technique was used for phase identification.
- Scanning electron microscopy (SEM) was utilized for post-experiment membrane analysis.
- The Energy dispersive spectrum (EDS) feature used with SEM, under the back-scattered electron (BSE) mode, provided improved compositional data.
- Quantometer analysis (optical emission spectroscopy) and the Inductively coupled plasma technique (ICP) were used for metal and electrolyte chemical composition analysis.

3.3 Initial bench-scale trials with chloride electrolyte system

A woven graphite cloth with 0.02 in (0.05 cm) nominal thickness and > 90 % porosity was selected as the first membrane material. To validate findings from previous work, the trials were started by using the LiCl-10 wt. % $AlCl_3$ electrolyte system. The simulated scrap for the first shake-down run (Run 1) employed Al-4.7 wt.% Si alloy. From this first trial we learned:

- The electrolyte has to be pre-formulated (by premelting $AlCl_3$ with LiCl to form a precursor of $LiAlCl_4$ according to the LiCl-AlCl3 phase diagram [6]). This is to avoid sublimation of $AlCl_3$ prior to start-up.
- The membrane fixture was modified to avoid detachment from the anode assembly.

Run 2 and Run 3 also investigated Al-4.7 wt.% Si alloys, while Run 4 was with Al-2.0 wt.% Cu alloy. Subsequent analysis posed the questions:

- Was current too low (below 10 A, see Figure 3) due to large anode-cathode distance (ACD)? or
- Was voltage too high due to an unidentified resistance?

[1] ATJ represents a commercial graphite grade.

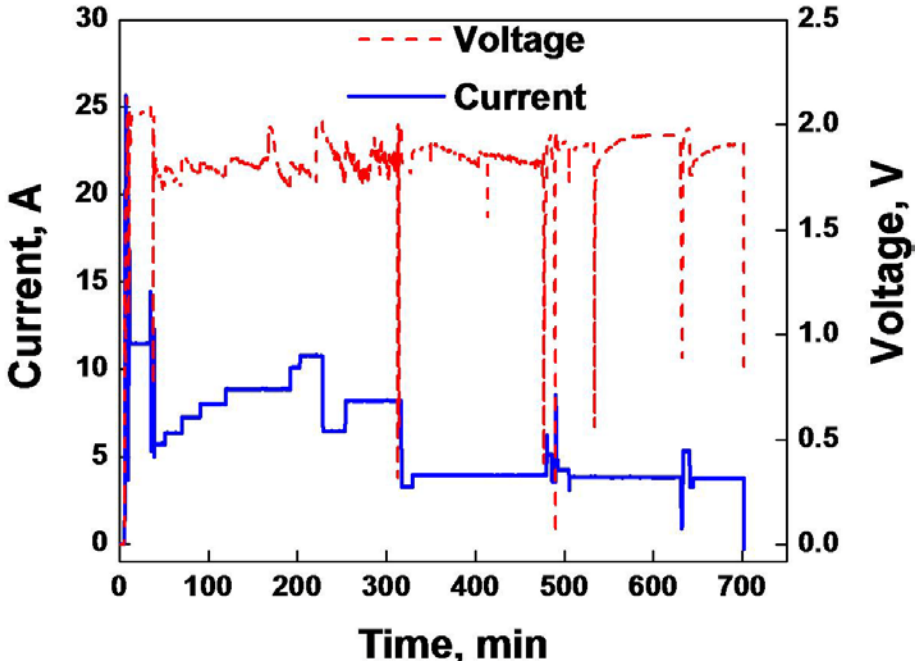

Figure 3 - Current and voltage traces for Run 4.

The runs also provided important information on cell operations:

- First, it was shown that a voltage ceiling must be imposed to avoid $AlCl_3$ decomposition into Al and Cl_2. According to a FactSage calculation (v. 6.2), at 700°C, the decomposition voltage of $AlCl_3$ is 1.85 V. This establishes the upper voltage limit where an $AlCl_3$-containing electrolyte could be stable.
- Secondly, the ACD should be controlled to avoid high resistance and attain appropriate current density. For the LiCl-10 wt.% $AlCl_3$ electrolyte system, the best range is from 0.5 in (1.27 cm) to 0.8 in (2.02 cm).
- Thirdly, $AlCl_3$ concentration was monitored and found to decrease appreciably with time. This provided the basis for the $AlCl_3$ replenishment rate for later trials. The root causes are not clearly understood but presumably related to the evaporation of $AlCl_3$ species.

3.4 Continued purification tests with chloride electrolyte system

Runs 5 through 13 were carried out with the graphite cloth membrane and the LiCl-10 wt.% $AlCl_3$ electrolyte to achieve stable cell performance and satisfactory purification results on Al-Cu, Al-Si, Al-Fe, and simulated brazing sheet scrap alloys. Respective results and remarks for each run are summarized in Table 2.

Table 2 - Results of experiments conducted in LiCl-10 wt.% $AlCl_3$ electrolyte

Run # (**Initial impurity, wt. %**)	**Final anode alloy impurity, wt.%**	**Final cathode alloy impurity, wt.%**	**Purification factor**	**Remark**
5 (Al-2.03Cu)	4.70	0.018	113	Poor cathode metal coalescence
6 (Al-4.73Si)	5.29	0.170	26	Poor cathode metal coalescence
7 (Al-0.58Fe)	0.60	0.300	2	Possible shorting
8 (Al-2.03Cu)	2.50	0.001	2030	Poor cathode metal coalescence
9 (Al-2.03Cu)	5.50	0.043	47	--
10 (Al-0.58Fe)	1.60	0.006	97	--
11 (Al-4.73Si)	--	--	--	Possible shorting
12 (Al-4.73Si)	2.90	0.100	47	Possible membrane leak
13 (Al-2.84Si-0.74Fe-0.80Mn)	3.32 (Si)	0.011 (Si)	258 (Si)	Low current density
	0.86 (Fe)	0.012 (Fe)	62 (Fe)	
	0.83 (Mn)	0.002 (Mn)	400 (Mn)	

For Run 5 the connection between the graphite cloth membrane and the anode chamber was improved. Though the initial stage current was low and voltage was not stable (Figure 4), it was found that after bubbling Argon into the anode alloy layer (at minute #630), cell current experienced sudden increase, and kept increasing with time. Concurrently, total cell voltage tended to decrease. The effect of Ar introduction is not thoroughly understood yet, but it is theorized that it might help break off the oxide layer deposited on the membrane.

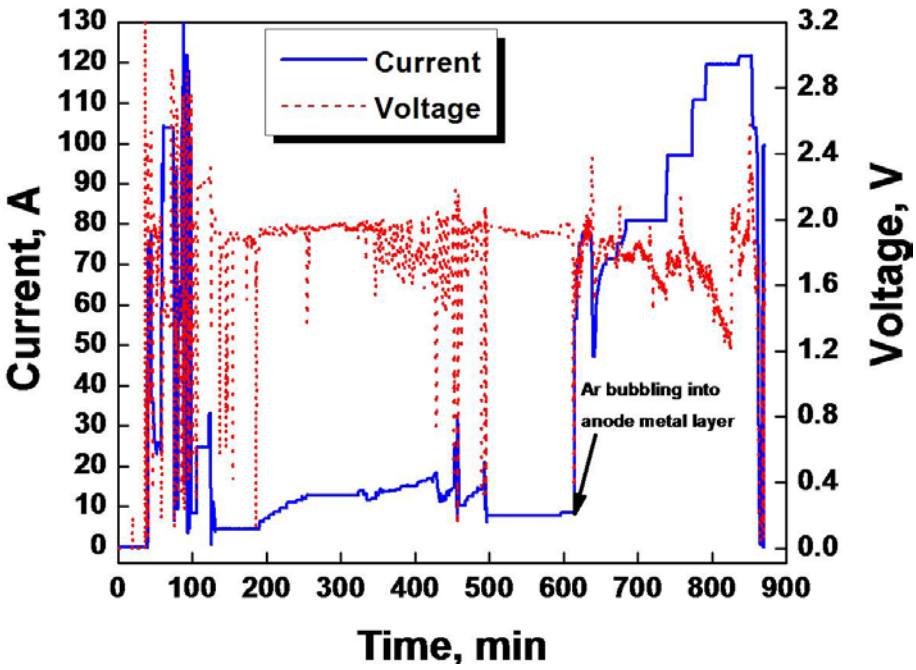

Figure 4 - Current and voltage trends for Run 5.
Arrow shows when Ar was introduced into the anode alloy layer

Runs 6 through 13 were conducted on various simulated scrap compositions: Al- 4.73 wt.% Si, Al-0.58 wt.% Fe as well as Al-2.84 wt.% Si-0.74 wt.% Fe-0.80 wt.% Mn. Each run's operation parameters (ACD, Ar bubbling rate, cell temperature) were kept as constant as possible.

Certain runs, for example Run 13, suffered from unstable cell performance. Figure 5 shows the current and voltage traces for Run 13, which, however, still yielded good purification results.

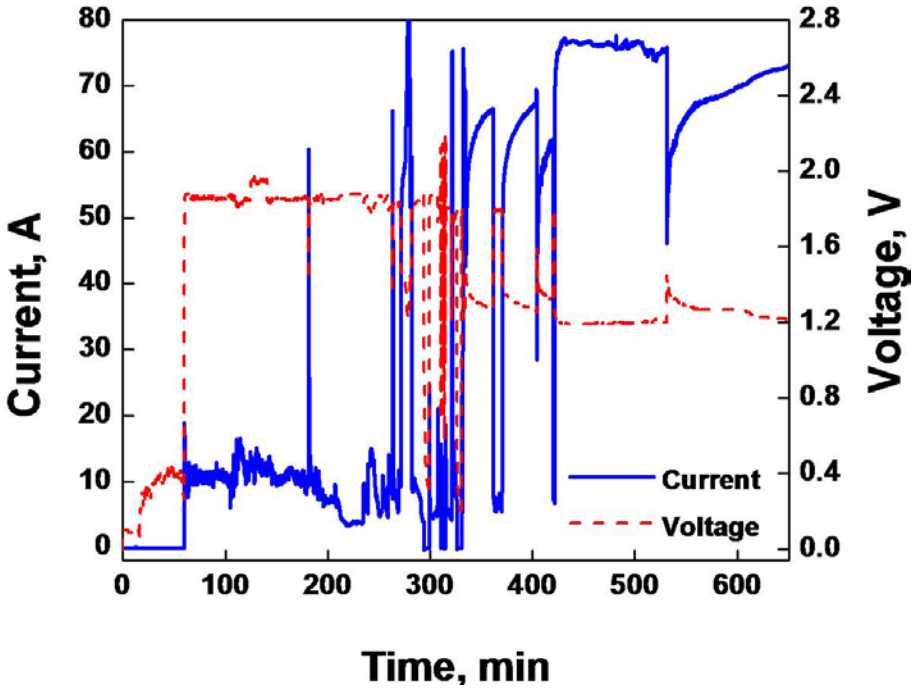

Figure 5 - Current and voltage traces for Run 13

In order to understand the poor cell performance, the membrane from Run 13 was analyzed through SEM-EDS. Figure 6 shows the morphology and corresponding spot analyses of the membrane. Both the original filament, and its adjacent regions are covered with deposits. From EDS examination, it was found that these spectra contain primarily Al and O peaks, suggesting the presence of pure Al_2O_3. Thermodynamic calculations indicate that the formation of Al_2O_3 is possible through the reaction between $AlCl_3$ and H_2O at 700 °C (forming Al_2O_3 and HCl).

However, the other possibility is that the Al_2O_3 came from the alumina thermocouple protective tubes and alumina liners and deposited on the membrane during the purification process. It should be noted that although Li is too light to be detected under EDS mode, Li_2O would not exist since its formation is not thermodynamically favored.

The current hypothesis is that alumina deposits blocked the membrane, hampering the purification process. The introduction of Ar into the anode alloy layer then helped break the alumina layer, and facilitate the cell performance.

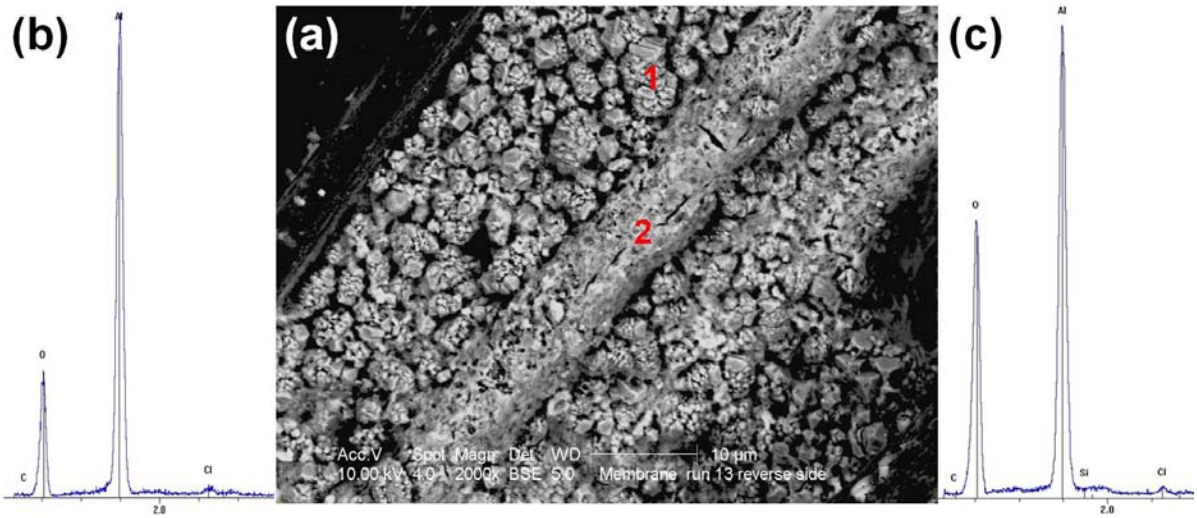

Figure 6 - Integrated SEM-EDS analysis on the graphite cloth membrane from Run 13. (a) Morphology of membrane filaments and alumina clusters; (b) and (c) are EDS spectra of spot 1 and 2, respectively

A common feature of the trials with a pure chloride electrolyte is the poor coalescence of the purified product. An example of metal recovered from Run 5 is shown in Figure 7. As can be seen in the picture, purified aluminum beads vary in size, tend to be suspended in the liquid electrolyte and do not settle down to coalese on the cathode aluminum pad. Based on previous smelting experience, an alternate electrolyte system using a fluoride addition was suggested to promote purified product coalescence and possibly better current efficiency of the entire purification process. The effect of small additions of AlF_3 on metal coalescence is supported by previous studies [7, 8].

Figure 7 - Uncoalesced aluminum beads from Run 5 obtained from thorough electrolyte dissolution with water. The beads are sitting atop the solidified cathode aluminum pad

3.5 Purification tests with fluoride-chloride electrolyte system

Runs 14 through 20 were tests conducted with a LiCl-10 wt.% $AlCl_3$-5 wt.% AlF_3 electrolyte. Purification results and features of each experiment are listed in Table 3.

Table 3. Results of experiments conducted in LiCl-10 wt.% AlCl3-5 wt.% AlF3 electrolyte

Run # (Initial impurity, wt.%)	**Final anode, Impurity, wt.%**	**Final cathode, Impurity, wt.%**	**Purification factor**	**Remark**
14 (Al-2.03 Cu)	2.30	0.12	**17**	--
15 (Al-2.03 Cu)	--	--	--	Graphite cloth membrane lost
16 (Al-2.03 Cu)	3.10	0.96	**2**	16 (graphite cloth membrane) and 17 (drilled rigid membrane, 0.8 mm thickness) shared same salt flux and cathode metal
17 (Al-2.03 Cu)	3.40			
18 (Al-2.84Si-0.74Fe-0.80Mn)	Si 16.0	0.80	**3.5**	Two days operation with 0.8 mm thickness drilled rigid membrane
	Fe 4.10	0.30	**2.5**	
	Mn 3.40	0.58	**1.5**	
19 (Al-2.03 Cu)	--	--	--	0.8 mm thickness drilled rigid membrane failed
20 (Al-2.03 Cu)	3.40	0.01	**203**	3.0 mm thickness drilled rigid membrane lasted four days

During Run 14, the first test with the new electrolyte , the current and voltage did not experience severe fluctuations as in Run 13, and the final product coalesced well with the aluminum pad, indicating that the minor addition of AlF_3 improved performance.

Detailed SEM-EDS investigations were carried out on the graphite cloth membrane retained from Run 16. Representative membrane filament morphology and EDS are shown in Figure 8. Unlike Figure 5, the membrane was not covered with thick solid alumina layers; instead, the spot analysis on one filament shows peaks of C (from filament itself), O, Al and Cl. The most probable explanation is that a certain amount of $AlCl_3$ remained on the graphite cloth, and, due to its hygroscopic nature, easily got dehydrated when exposed to atmosphere..

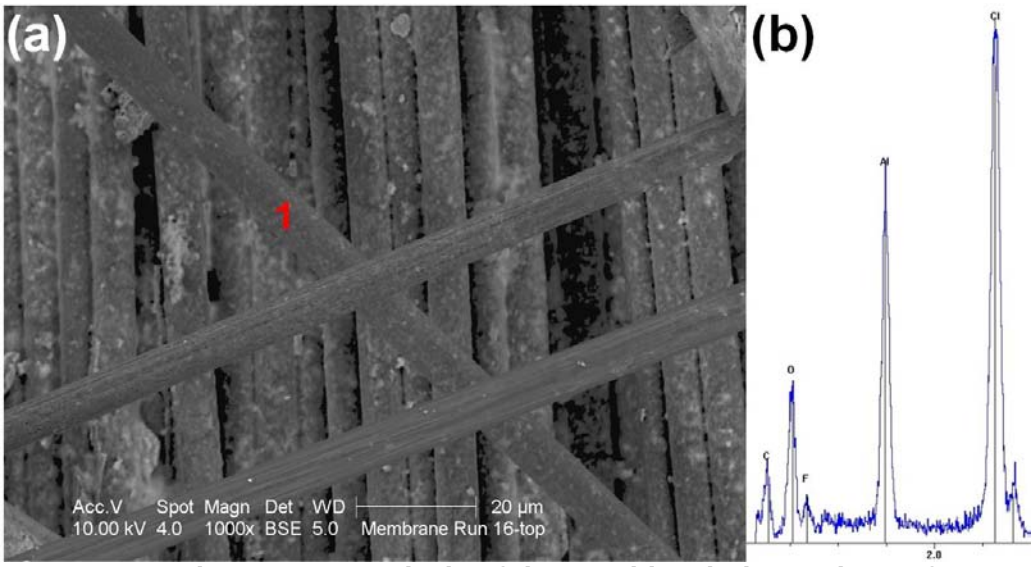

Figure 8 - Integrated SEM-EDS analysis of the graphite cloth membrane from Run 16. (a) Morphology of membrane filaments and (b) corresponding energy dispersive spectrum for Point 1

Run 17 was the first test to use the alternate graphite drilled rigid membrane. The drilled rigid membrane (See Figure 9) has a nominal porosity of 33%, and is composed of 1,314 uniformly drilled holes, 0.8 mm in diameter.

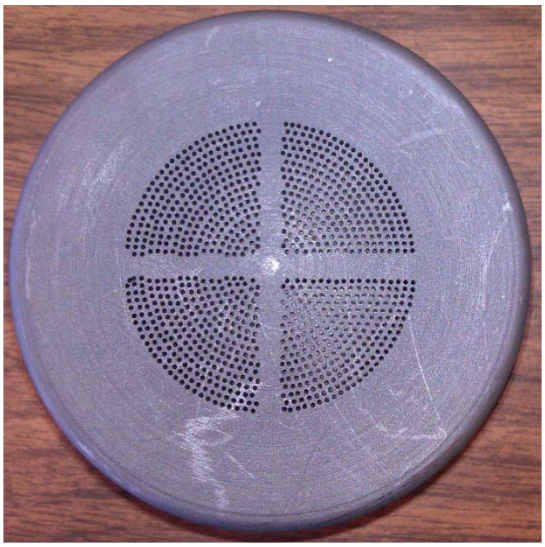

Figure 9 - Drilled rigid graphite membrane.
Note: The unperforated cross-shaped area was designed for mechanical strength

Figure 10 shows current and voltage results for Run 17. It is clear that both voltage and current exhibited a much more stable behavior as the experiment progressed. Voltage was controlled below 1.85 V and current was in the range of 35 ~45 A. Final anode impurity levels were close to theoretical predictions and Al coalesced well with the aluminum pad in the cathode.

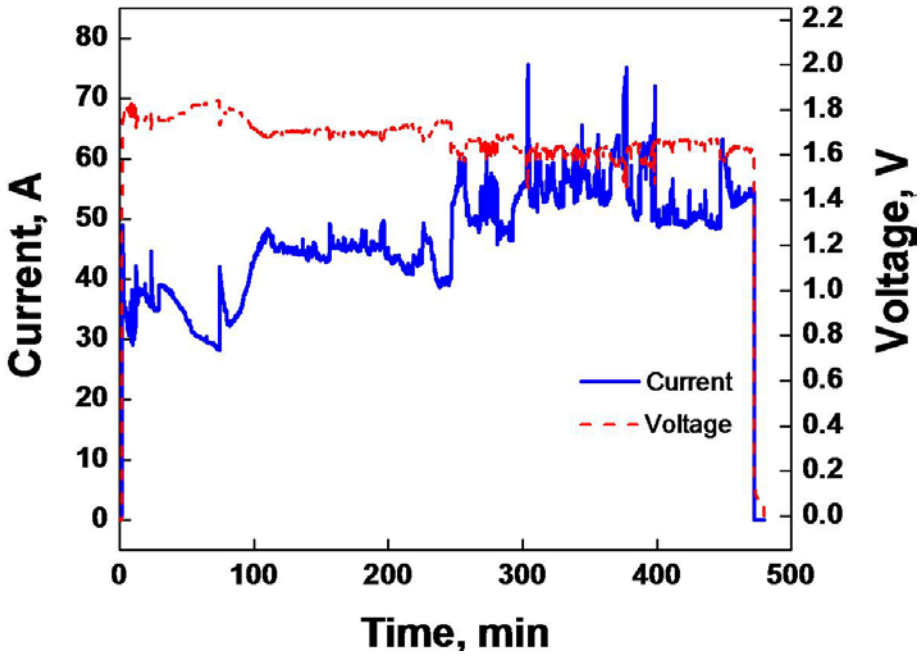

Figure 10 - Current and voltage traces for Run 17

Run 18 and Run 19 were planned to achieve longer duration tests with the 0.8 mm thickness drilled rigid membrane. A simulated brazing sheet composition (Al-2.84 wt.% Si-0.74 wt.% Fe-0.80 wt.% Mn) and Al-2.03 wt.% Cu alloy, respectively, were purified. Run 18 ran successfully with two days stable operation. The membrane broke during Run 19 prompting a change in design to a thicker, 3.0 mm rigid membrane.

Run 20, with the thicker rigid membrane, ran for four days as shown in Figure 11. Except for some transient hikes, cell current remained in the range of 35~45 A.

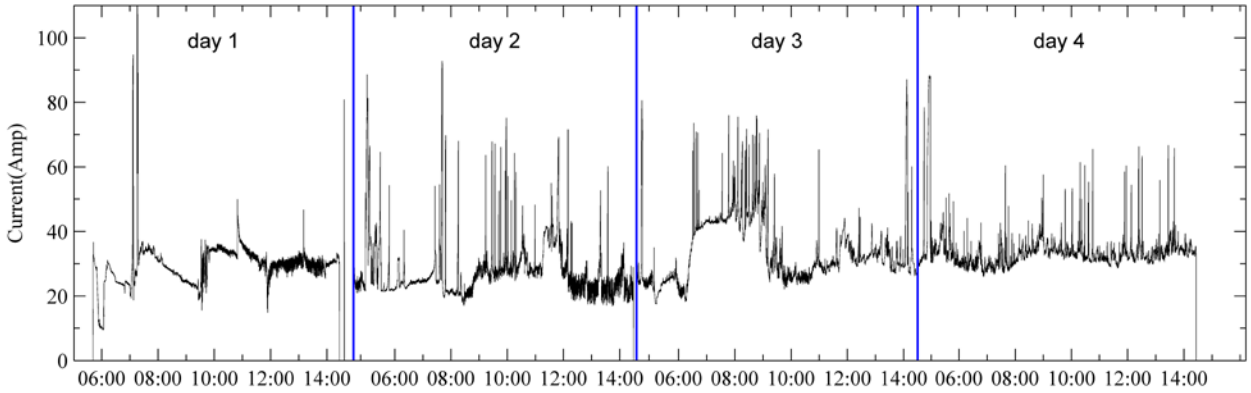

Figure 11 - Current trace for Run 20
Note: Individual day's operation are separated by blue lines

As part of the investigation, the ACD (anode-cathode distance) vs. voltage and ACD vs. current relationships were investigated. See Figure 12. The data was compared to the similar study by Bowman [9]. Cell current (or current density) is decreasing virtually linearly with increasing ACD, while cell voltage increases with increasing ACD. Current density was comparable to one of Bowman's test cases at ~3 A/cm^2.

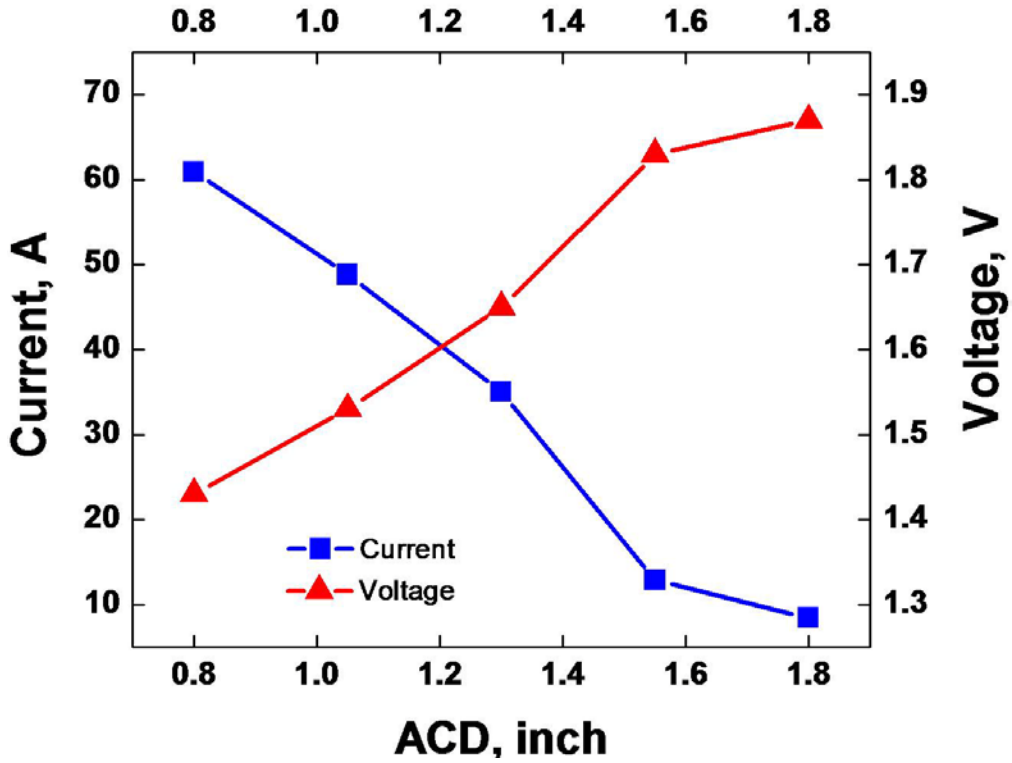

Figure 12 - Cell current and voltage as a function of Anode-Cathode Distance (ACD)

3.6 Purification tests with pure fluoride electrolyte system

An alternative electrolyte was investigated as the chloride electrolyte system suffered from a high evaporation rate, driving the need for frequent replenishment. Moreover, it was demonstrated that an addition of AlF_3 significantly promoted aluminum coalescence at the cathode and minimized the formation of aluminum oxide deposits on the membrane. Therefore, on all fluoride electrolyte system, LiF- 10 wt.% AlF_3, was selected for further investigation.

For the LiF-10 wt.% AlF_3 system, the operating temperature should be above 860 °C [10], and the density at that temperature is 1.861 g.cm-3, close to that for the LiCl-10 wt.% $AlCl_3$ system. The specific conductivity of LiF is 8.0 Ω-1cm-1[11, 12], while that of LiCl is 6.31 Ω-1cm-1. Therefore, the fluoride-based electrolyte should provide similar conductivity performance as the chloride-based electrolyte. Since LiF and AlF_3 have relatively low volatility electrolyte evaporation should be reduced and this should eliminate the need for constant salt charging to compensate for any losses.

Runs 21 and 22 were two and three day tests respectively using the new electrolyte.

Figure 13 shows the recorded cell current trace of Run 21. It can be seen that for Day 1 operation, cell performance was stable at the expected current reading around 45 A. However, after only two hours of relatively stable operation from Day 2, cell performance gradually deteriorated even though ACD was adjusted, Ar bubbling was introduced into the anode metal layer, and the electrolyte was stirred.

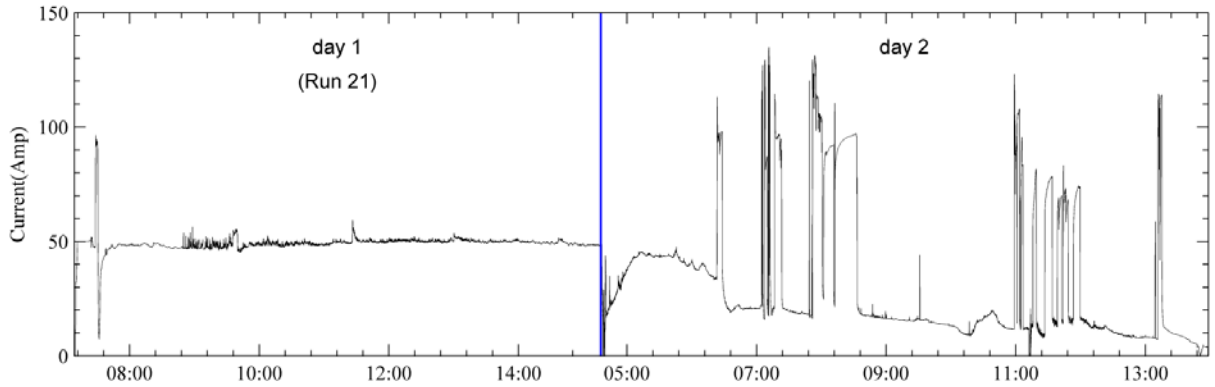

Figure 13 - Cell current trace for Run 21.
Note that individual day's operation is separated by blue lines.

It was also noticed that with cell performance deteriorating, the anode reference electrode voltage reading (Figure 14) increased, indicating an ever increasing anode resistance.

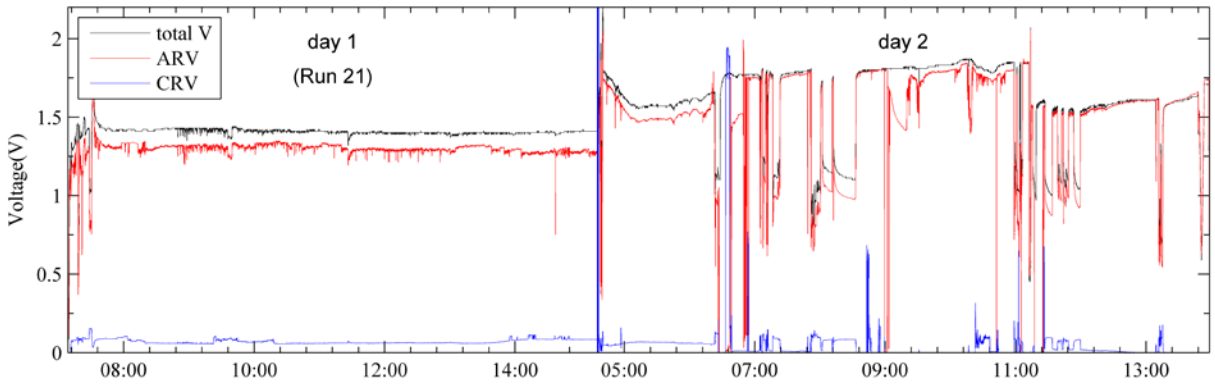

Figure 14 - Cell voltage traces for Run 21.
Total voltage in black, anode voltage (ARV) in red and cathode reading (CRV) in blue

After Run 21, the anode was replaced with fresh Al-2.03wt.% Cu alloy. The purification process was resumed the next day as Run 22, without changing the electrolyte and graphite crucibles. Run 22 lasted for three days.

Post experiment autopsy of the anode from Run 21 revealed that both bottom and top surface of the membrane were severely clogged by thick layers of deposits as shown in Figure 15. Figure 16 shows the SEM-EDS examination of the clogged membrane. 16(a) shows the boundary between a clogged drilled hole and the adjacent plugged graphite substrate. Both regions are covered with dense deposits, which are featured in 16(b) and 16(c) at higher magnification. EDS analysis results are listed in Table 4.

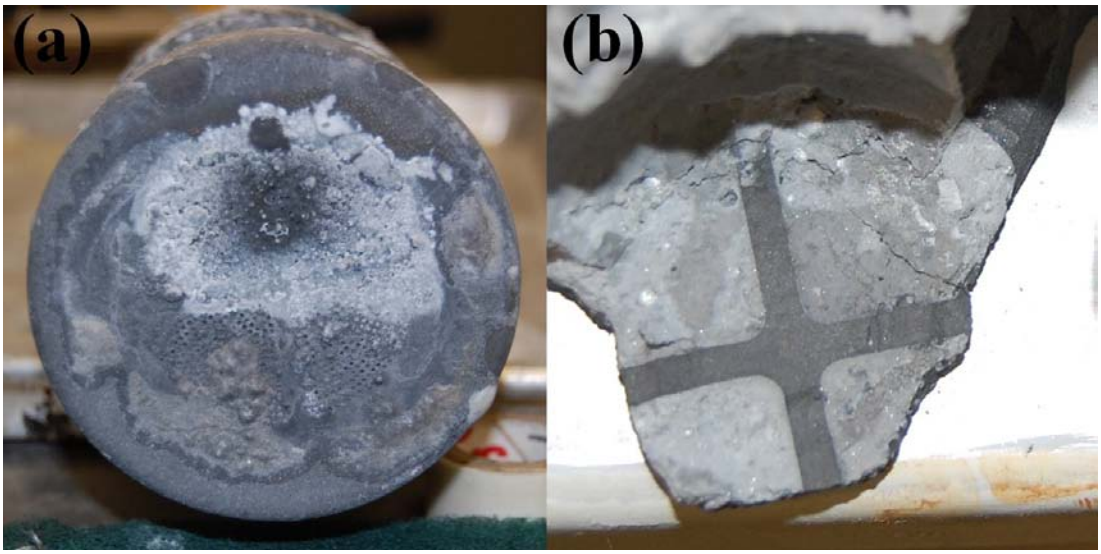

Figure 15 - Run 21 post experiment membrane
(a) bottom view and (b) top (inside the anode) view
Dark-grey cross is the graphite reinforcing ridge to strengthen the membrane

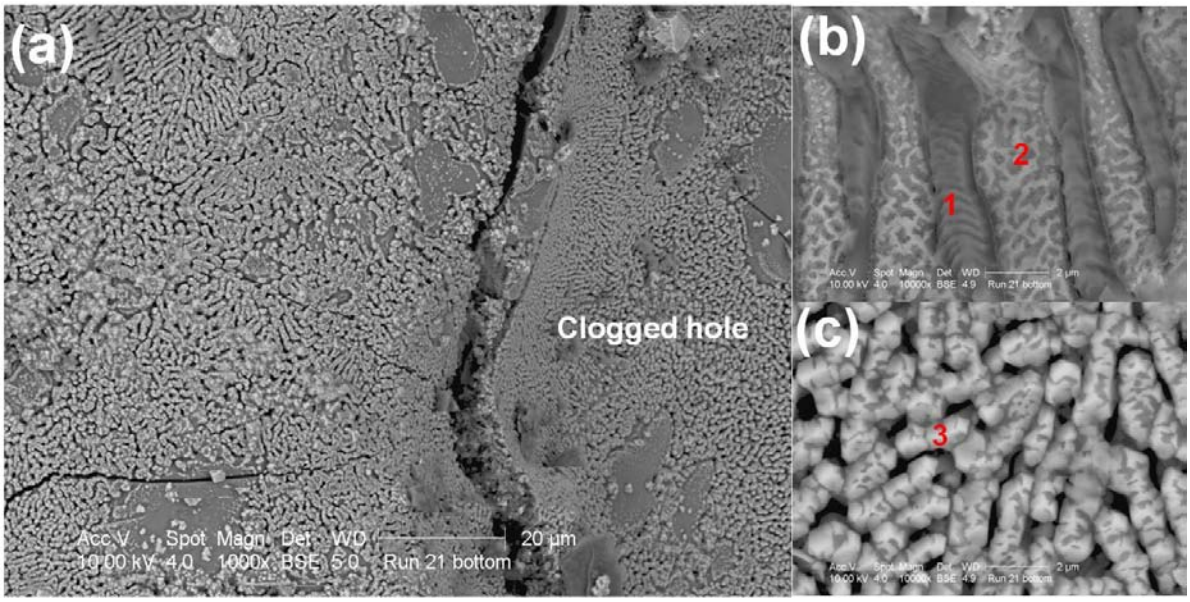

Figure 16 - SEM examination of the clogged membrane from Run 21.
Red numbers correspond to areas where EDS were conducted.

Table 4 - Quantitative EDS analysis of Run 21 membrane deposits

Point	Al, at.%	O, at.%	F, at.%
1	0.85	--	99.15
2	11.80	0.33	87.87
3	3.65	15.24	81.11

As noted in Table 4:

- Point 1 primarily consists of F peak, most likely pure LiF.
- Point 2, in addition to F, involves a certain amount of Al, most likely a mixture of LiF+AlF_3
- Point 3, in addition to F, involves a certain amount of O, most likely a complex Li-Al-O-F compound or a mixture of compounds.

All of these phases were verified using X-Ray Diffraction (XRD) which indicated the major phases as C, AlF_3, Li_3AlF_3 and $LiAl_5O_8$.

An autopsy of the unit following termination of Run 22 showed that the alumina liners protecting the anode were missing, and that the electrode reference voltage and Ar bubbling alumina tubes had shrunk in diameter. It is believed that the alumina dissolved into the fluoride-based electrolyte. However, the total amount of lost alumina is higher than the dissolved amount based on solubility considerations [13, 14] and on calculations from LECO oxygen analysis. Since both the EDS analysis and XRD examination provide evidence for the formation of Li-Al-O-(F) complex phases, it is likely that a certain amount of alumina has reacted with the electrolyte as suggested by previous researchers [15, 16].

Regarding overall cell performance in the late stages, it is believed that the electrolytic process was affected by non-dissolvable deposits that clogged the membrane holes. Continued studies on deposit formation mechanisms are needed to substantiate further applications of fluoride based electrolytes. For example, experiments should be conducted without using alumina ceramics in the system. Some alumina stability tests should be conducted with various fluoride salt compositions, to identify more suitable electrolyte compositions.

3.7 System mass balance

One issue that was identified during the study was the total aluminum mass balance, i.e. the ratio between the Al input and the Al recovered from the cell. The input feed sources included the anode alloy charge and initial Al charge to the cathode pad. The recovered Al consisted of the Al charge remaining in the anode, the final cathode Al pad, the Al beads recovered from the electrolyte, as well as the sum of samples obtained during the experiment for chemical analyses. The recovered Al ranged from 92.7 to 97.4 % of the input Al, excluding runs 21-22, which were atypically low at 85 %. The average recovery for runs 5 through 20 was 95.0 %.

Table 5 lists the mass balance of each experiment starting with Run 5. The total metal weight loss in the third column is calculated from the difference between the total Al input and the total Al output. The percent recovery is shown in column four. The next two columns exhibit the actual anode charge weight change, which is a good indicator of how much Al alloy has been electrolytically purified, and the theoretical weight change based on Faraday's Law.

Table 5 – Mass Balance Numbers for Tests 5 - 22

Run	Total Metal Input (g)	Total Metal Output (g)	Total Metal Loss (g)	Recovery (%)	Anode Alloy Weight Change (g)	Theoretically Transferred Mass (g)	Remark
5	1752.24	1647.10	**105.14**	**94.0**	141.00	183.60	--
6	1912.42	1862.85	**48.57**	**97.4**	72.06	290.18	Additional alloy charge, shorting
7	1750.15	1630.60	**119.55**	**93.2**	21.61	160.07	Shorting, metal samples taken during experiment
8	1751.34	1655.13	**96.21**	**94.5**	25.27	165.24	
9	1750.75	1651.30	**99.45**	**94.3**	233.97	169.18	Possible membrane leak
10	1755.50	1664.64	**90.86**	**94.8**	194.56	143.40	--
11	1801.30	1740.49	**60.81**	**96.6**	46.59	248.40	Additional alloy charge, no Al beads, shorting
12	1751.22	1667.77	**83.45**	**95.3**	240.38	78.83	Possible membrane leak
13	1751.92	1666.64	**85.28**	**95.1**	18.36	147.20	Possible shorting
14	1750.14	1696.04	**54.10**	**96.9**	69.04	66.67	--
15	1751.30	1670.05	**81.25**	**95.4**	--	54.76	Missing membrane
16	2001.05	1879.14	**121.91**	**93.9**	128.85	100.01	Cloth membrane
17					126.45	123.62	0.8 mm rigid membrane
18	1820.14	1708.86	**111.28**	**93.9**	283.35	274.03	2-day run
19	3615.36	3484.72	**130.64**	**96.4**	--	--	4-day run; two membranes missing
20	2196.00	2036.23	**159.77**	**92.7**	426.1	402.61	4-day run
21	2133.29	1814.40	**318.89**	**85.0**	208.78	230.2	21 (two days) and 22 (three days) share same electrolyte flux and cathode metal; anode changed
22					242.62	280.61	

The following mechanisms could contribute to the metal "loss":

1. Unretrievable metallic aluminum. This could result from the following possible reasons:
    a. Manual handling of the cell - during autopsy, the cell is broken apart manually, and it is impossible to recover 100% of the metallic Al beads in the cell using the manual separation techniques.
    b. Al attaching to the graphite walls - Al still remains mechanically attached to the graphite walls after manual breaking. It is difficult to retrieve all of the metal that is adhered to the debris.

    It is thought that these types of losses could account for 10 to 20g of aluminum, but it is hard to imagine that 100g of aluminum could be lost in this way.
2. Reaction of Al with graphite - at 700 ^{o}C (close to the cell operating temperature), the aluminum-carbon reaction:

    $$4Al + 3C \rightarrow Al_4C_3$$

    shows a large negative Gibbs Free Energy value of -176.9 kJ/mole, which indicates that the formation of Al_4C_3 is thermodynamically possible. Past experience, though, is that in practice the reaction progresses at a very slow rate.
3. "Gray layer" formation – for several experiments a gray layer was found in between the bulk electrolyte and the cathode Al layer. For example, an analysis of Run 14 found that up to 10 wt.% of the layer was insoluble.The XRD and free metal analysis suggests that major phases are AlF_3 and Al_2O_3 and Al.

As seen in Table 5, in tests that showed no indications of shorting or membrane breech, (Runs 14, 16, 17, 18, 20, 21 and 22), the actual anode charge weight change agrees fairly well with the theoretically transferred weight. The ratio between the actual anode charge weight change and the theoretically transferred weight is one measure of cell efficiency. In the afore-mentioned experiments the efficiency by this measure is close to 100%. This suggests that the issue with mass balance closure is not due to the anode.

It should be noted that for runs having significantly reduced current efficiency (Run 6, 7, 8, 11, and 13), shorting appeared to have occurred; for runs having far more than 100% current efficiency (Run 9, and 12), the membrane for each test was found missing, indicating bulk flow of metal out of the anode.

Based on the above observations and discussion the following tasks are suggested to improve the mass balance closure.

a. The chemistry of the previously identified gray layer for each individual run needs to be fully analyzed and the mechanisms need to be understood.
b. The cathode graphite chamber internal side walls should be shielded with a boron nitride lining to prevent reaction of Al with graphite.
c. The electrolysis experiments need to be run for longer durations to determine if the mass balance closure improves as more aluminum is purified. The weight of unrecovered beads in the electrolyte should be approximately constant, and thus on a percentage basis should decrease as the weight of the aluminum processed increases.

4.0 Economic Assessment

This assessment will review the United States scrap market and the economic viability of the membrane cell to purify that scrap. Scrap prices and volume sold are quantified for January 2010 to August 2011. Two different cases are assessed: 1) purify low value scrap sold on the U.S. market and 2) produce high purity aluminum. The economic benefit for utilizing waste heat from the membrane cell to melt aluminum is also quantified.

The economic viability of the membrane cell to purify scrap is sensitive to primary & scrap aluminum prices, and the cost of electricity. In particular, the differential between scrap and primary aluminum price which is highly variable and dependent on the scrap source. In order to be economically viable, any scrap post-processing technology in the U.S. market must have a total operating cost well below the scrap price differential of $0.20-$0.40 per lb to the London Metal Exchange (LME), a margin of 65%-85% of the LME price.

4.1 U.S. market conditions

Figure 17 shows primary aluminum price, both U.S. Midwest market price and LME Grade A cash price, for the time period from January 2010 to July 2011. The Midwest market price had a margin approximately 6% greater than LME for the 19 month duration.

Figure 18 shows the price differential for several scrap streams: used beverage cans (UBC), mixed low copper clips, old sheet/castings, and turnings (clean and dry). Old sheet/castings and turnings have the largest price differential at approximately $0.34 per lb below primary aluminum (a margin of 70% of LME). Mixed low copper clips and UBC compete for the lowest price differential. In July 2011 UBC was the most valuable scrap stream at approximately $0.24 per lb below LME (a margin of 78% of LME) followed by mixed low copper clips at $0.28 per lb below LME (a margin of 75% of LME).

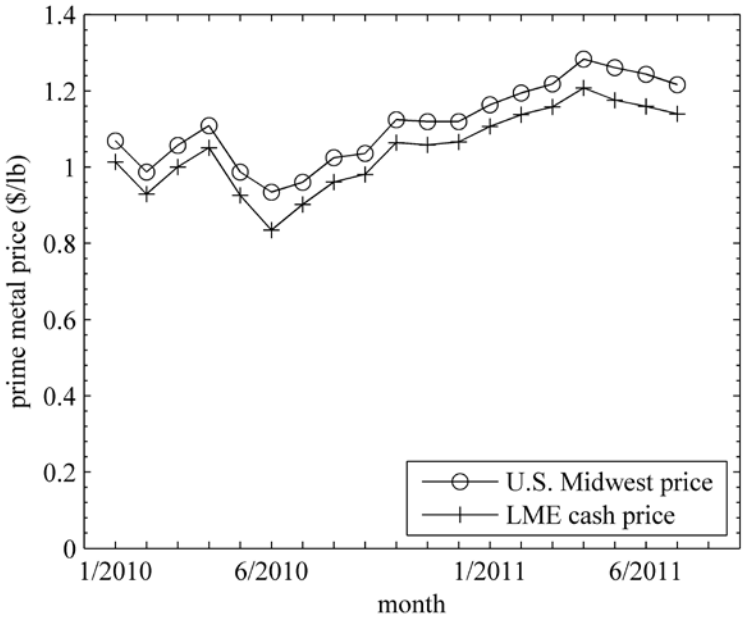

Figure 17 - Primary aluminum prices from January 2010 to July 2011 (U.S. Midwest market price and LME Grade A cash price).

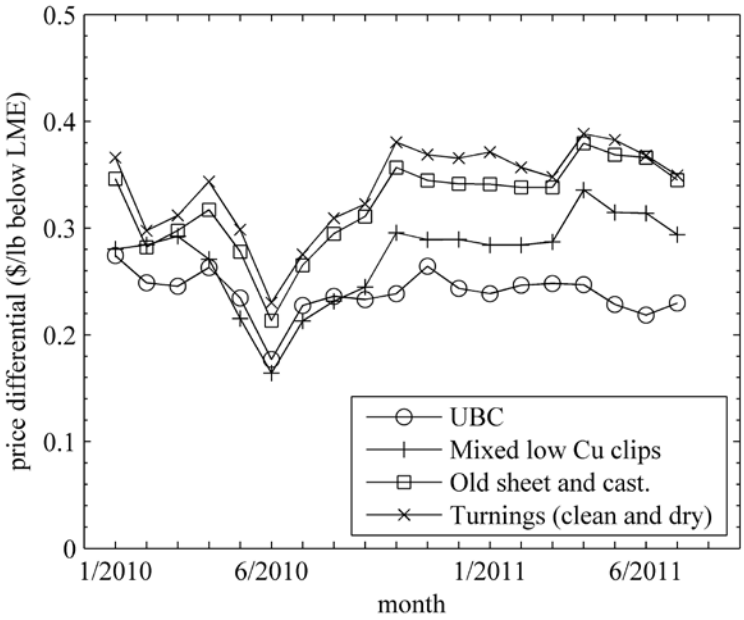

Figure 18 - Scrap price differential ($ per lb below LME) for several scrap streams: used beverage cans (UBC), mixed low copper clips, old sheet/castings, and turnings (clean and dry).

4.2 Process costs: Energy and Materials

The equations below describe the performance of the membrane cell: The first equation describes electricity costs per mass purified. The second equation describes the value per mass produced, based from the cost of scrap, value of product and value of the metal left in the anode. The electricity cost per mass purified is derived from the energy required to purify a unit mass of aluminum and the electricity costs. The energy required to purify a unit mass of aluminum is derived from Faraday's Law and the current efficiency of the cell.

$$c_e = C_e \frac{VnF}{\varepsilon_j AW_{Al}}$$

$$v = v_p + v_d \frac{1 - r_p}{r_p} - \frac{c_s}{r_p}$$

The material cost and maximum value generated by purification is shown in Table 6 for two cases. The first case is to purify low cost scrap having a cost of $0.40 per lb below LME (a margin of 65% of LME), and results in a material value increase of $0.30 per lb purified. The second case is to produce high purity aluminum from primary aluminum. The processed product is expected to have higher purity than primary, therefore the purified product can be sold as a value-added product in the market. The product recovery is also expected to be greater for high purity production because the starting feedstock contains fewer impurity elements. The high purity aluminum market is quantified in Bryant [17] and can be as high as $0.40 per lb above LME. The value of the downgrade is assumed to be $0.00 in the three cases. Ideally, concentrated alloying elements in the downgrade metal could be reused, and the downgrade would have value.

Table 6 - Material cost and value increase by purification for two cases.

Material costs	Purify low value scrap	Produce high purity from primary aluminum
Feedstock cost ($/lb)	$0.74	$1.14
Downgrade value ($/lb)	$0.00	$0.00
Purified product value ($/lb)	$1.14	$1.54
Purified Recovery (mass purified / mass feedstock)	0.88	0.95
Value increase ($/lb purified)	$0.30	$0.34

The estimated costs for a production cell are listed in Table 7. The estimates are determined using the proposed production cell discussed in Martchek [3]. Briefly, the production cell has an overall production capacity of 70,000 lb per day at current density of 20 A/in^2 (3.1 A/cm^2). The infrastructure components are updated from 1981 to 2010 to account for currency inflation of 237%.

Energy consumption estimated for the proposed production cell, based on our experimental data, is shown in Table 8. The estimates are calculated using 2011 industrial electric prices as quantified by Energy Information Administration. The proposed production cell aims to decrease the operating voltage by reducing the anode-cathode distance (ACD). This results in lower energy consumption on a per mass basis as defined by the equation below (the energy required to purify).

$$E = \frac{VnF}{\varepsilon_j A W_{\mathrm{Al}}}$$

There is an anticipated energy savings when comparing the membrane cell technology from this study to the Hoopes cell to produce high purity aluminum and replace primary aluminum used as sweetener to recycle scrap. The laboratory scale membrane cell used in this investigation purified aluminum at an energy cost of 2.9 kWh/lb (not including external heating required to maintain the cell temperature), a 36% savings over the Hoopes cell and primary aluminum production energy cost of 8 kWh/lb.

Energy costs for the membrane cell can be reduced in two ways: improve current efficiency and reduce cell operating voltage. The proposed production cell, listed in Table 8, is the future development goal. It is anticipated the current efficiency can be increased from 70% to 90% and the operating voltage can be decreased from 1.5 V to 0.6 V. If these goals can be achieved, the energy required to purify aluminum would be reduced to 0.9 kWh/lb, which is 11% of the Hoopes cell and primary aluminum production energy cost.

Table 7 - Infrastructure costs
Projected capacity - 70,000 lb/day (11,550 tonne/yr)

Infrastructure	**Cost (K)**	
Steel Shell	$2,360	
Refractory insulation	$1,560	
Graphite: - cathode and anode crucibles - membrane	$3,040	
Electric supply	$3,180	
Material handling: - scrap charging - product removal	$660	
Building space	$3,570	
Misc.	$64	
Total for Infrastructure	**$14,434**	
Infrastructure conversion cost	**$0.56 $/(lb/yr)**	**$1,250. $/(tonne/yr)**

Table 8 - Experimental and projected energy cost for the purification cell.

		Experimental measurements	**Projected**
		1.5 V, 2.4 A/cm^2	0.6 V, 3.1 A/cm^2
ACD	(mm)	16	6
Electrolyte resistivity	(ohm cm)	0.38	0.33
Power requirement *	kWh/lb	2.9*	0.9**
	kWh/tonne	6400*	2000**
Power cost (at 0.05 $/kWh)	($/lb)	$145	$45
	($/tonne)	$320	$100
Capacity Assuming: 7.85 m^2 membrane area (one cell of 18 cell bi-polar design)	(lb/day)	3100	3900
	(tonne/yr)	510	650

*** Assumptions: 1) Current efficiency of 70% for the test cell**
2) Current efficiency of 90 % for the production cell

The process operating costs are shown in Table 9. The membrane cell is estimated to have an operating cost of approximately $0.181 per lb excluding interest, tax, depreciation and amortization. This value then provides the guideline for determining the profitability of the cell, not including additional benefits; e.g. it provides molten metal directly.

Table 9 - Process operating cost for the membrane cell.

	$/lb	$/tonne
Electrolyte	$0.012	$26.12
Cell lining	$0.024	$52.25
Repair & Maintenance	$0.024	$52.25
Labor	$0.071	$156.75
Electric power	$0.050	$110.23
Cost (excluding interest, tax, depreciation and amortization)	**$0.18**	**$397.60**

4.3 Economic benefit of using the membrane cell to both purify and to melt aluminum

There are two major benefits to using the membrane cell to melt aluminum. First, there is a melt loss savings when using the membrane cell, because the molten aluminum is not exposed to products of combustion as is the case for a natural gas fired furnace and the molten salt electrolyte protects the molten aluminum from the atmosphere. Second, when the electric resistance heat (I^2R) generated in the membrane cell is used to melt additional scrap, the operating costs on a per ton basis are reduced. Essentially, the membrane cell becomes both a purification system and a very efficient electric melting system. If the excess heat in the system is used so that for every lb of Al purified an additional 2 lb of Al is melted, the overall costs are reduced to less than the cost for melting in a gas-fired reverberatory furnace.

Table 10 gives the basic prices and costs used to estimate the overall savings. For the membrane cell costs two scenarios were used with a differing ratio of melted metal to purified metal. In one case this ratio was 1, meaning that all the metal added to the membrane cell was melted and purified. In the second case, this ratio was 3, meaning that the excess heat generated in purifying metal was used to melt additional metal. In other words, the I^2R heat of the membrane cell was used to melt additional scrap.

Table 10 - Price and Cost Data Used for Economic Calculations

	Basic Price/Cost ($/lb Al)	Data Source
Primary Aluminum Price	$1.08	LME, August 2011
Scrap Price (old sheet and castings)	$0.76	American Metal Market, August 2011
Gas-Fired Melting Cost	$0.05	Internal Alcoa Data
Membrane Cell Cost (Melted/Purified = 1)	$0.18	Estimated
Membrane Cell Cost (Melted/Purified = 3)	$0.06	Estimated

To estimate potential cost savings for the process, three cases were considered:

- For the Base Case, two-thirds of the total charge is scrap melted in a gas-fired reverberatory furnace, and one-third is primary metal, also melted in a reverberatory furnace. Melt loss for scrap melting in a reverberatory furnace is assumed to be 3.5%. Melt loss for melting primary metal is assumed to be 1%.

- For Membrane Cell Case I, two-thirds of the total charge is scrap melted in a reverberatory furnace and one-third of the charge is scrap melted and treated in the membrane cell. The melt loss and metal loss due to removal of concentrated impurity elements in the membrane cell for melting in the membrane cell are assumed to be 0.5% and 4.5% respectively, for a total loss of 5%.
- For Membrane Cell Case II, all of the charge is scrap melted in the membrane cell, one-third of which is also purified in the membrane cell.

Table 11 summarizes the estimated costs for the three cases. Membrane Cell Case I shows a $0.06 per lb cost savings from the Base Case, an 6% decrease. Membrane Cell Case II demonstrates a $0.08 per lb savings from the Base Case, a 8.5% decrease.

Table 11 - Estimated Cost Savings for Membrane Cell Purification and Melting of Scrap

	Metal cost ($/lb)	Process costs ($/lb)	% Metal Loss	Metal Loss Cost ($/lb)	Total ($/lb)
Baseline Case: 2/3 Gas-fired Al, 1/3 Primary Al					
Gas fired melting	$0.50	$0.03	3.5	$0.02	$0.56
Primary Aluminum	$0.36	$0.02	1.0	$0.005	$0.38
Total ($/lb)	$0.86	$0.05		$0.02	$0.94
Membrane Cell Case I: 2/3 Gas-fired Al, 1/3 Membrane Cell Al					
Gas fired melting	$0.50	$0.03	3.5	$0.02	$0.56
Membrane Cell	$0.25	$0.06	5.0	$0.01	$0.32
Total ($/lb)	$0.76	$0.09		$0.03	$0.88
Membrane Cell Case II: Membrane Cell Only					
Membrane Cell	$0.76	$0.06	5.0	$0.04	$0.86
Total ($/lb)	$0.76	$0.06		$0.04	$0.86

4.4 Economic assessment conclusions

Table 12, below, shows the earnings before interest, taxes, depreciation, and amortization (EBITDA) possible, without considering the benefits of melting:

- By purifying low value scrap ($0.40 per lb below LME), the membrane cell can generate a profit of $0.12/lb.
- By producing high purity from primary Al, the membrane cell can generate a value of $0.16/lb.

There are important challenges to consider when purifying low value scrap. Low value scrap streams are likely to have contaminants such as other refuse, and surface coatings. Additional equipment will be needed to remove these contaminants and will increase the process cost. Scrap sources will also be variable in volume, cost, and purity which all contribute to the risk of the opportunity. Operating cost data from other less risky implementations of the membrane cell would be useful to identify upper limits for the cost of the scrap cleaning processes.

If aluminum is increasingly used in the automotive market, it is possible for the scrap stream differential to consistently be greater than $0.50 below LME, the economics become favorable to using the membrane cell to purifying this scrap.

Table 12 - Net Earnings

	Purify low value scrap ($0.40 below LME)		Produce high purity aluminum	
	$/lb	**$/tonne**	**$/lb**	**$/tonne**
EBITDA value	$0.12	$265	$0.16	$350

5.0 Conclusions

The electrolytic purification process was demonstrated in a laboratory scale cell with a horizontal anode membrane. The process was tested using four different scrap alloy compositions, three different anode membranes and three different electrolyte systems. Cell voltage and current, operating temperature, and anode-cathode distance were measured. Based on the experimental results, the following conclusions are drawn:

1. The membrane cell purification concept has been validated on laboratory scale with successful runs on simulated scrap aluminum (Al-2.03 wt.% Cu, Al-4.73 wt.% Si, Al-0.58 wt.% Fe) and a brazing sheet scrap composition (Al-2.84 wt.% Si-0.74 wt.% Fe-0.80 wt.% Mn). Target purification factors >20 and purified products containing greater than 98 wt.% Al were repeatedly achieved for each of the elements in the respective alloys.
2. Three electrolyte systems: LiCl-10 wt.% $AlCl_3$ and LiCl-10 wt.% $AlCl_3$-5 wt.% AlF_3 and LiF-10 wt.% AlF_3 have been tested.
3. In pure chloride electrolytes alumina deposits were found to form and block the graphite cloth membrane and degrade the process.
4. Addition of 5 wt.% AlF_3 into the electrolyte eliminated aluminum oxide deposits on the membrane and allowed for stable performance for test durations of up to four days without degradation in cell performance.
5. The addition of AlF_3 also promoted coalescence of the purified product at the cathode avoiding electrical shorting and cell failure, further enhancing cell performance.
6. Stable cell performance was maintained at an anode current density at ~2.8 A/cm^2 and stable voltage of 1.62 V. The calculated energy requirement for the membrane electrolytic purification process was ~4.82 KWh/kg (assuming 100% current efficiency), which is less than one-third of the Hoopes Cell process.
7. A drilled rigid graphite membrane with reinforced thickness (3.0 mm) was selected as the most promising candidate compared to the graphite cloth and thin (0.8mm) rigid membrane.
8. In a pure fluoride electrolyte system, the cell performance was initially satisfactory, but became unstable afterward. The electrolytic process lasted up to three days but suffered from substantial clogging by a Li-Al-O-(F) complex phase deposit. Further investigation is needed to reveal the root causes for the formation of these phases.
9. The lab-scale membrane cell's total metal output is generally lower than the total metal input. This phenomenon might be due to unretrieved metal, possible aluminum reaction with graphite, and loss of aluminum in the formation of a gray layer on the cathode.
10. The cost to operate the membrane cell is estimated to be < $0.24/lb of purified. The energy cost is estimated to be $0.05/lb of purified with the remaining costs being repair and maintenance, electrolyte, labor, taxes and depreciation.
11. After successful future development, the membrane cell could potentially produce high purity aluminum having a value of $0.40/lb above LME.
12. A scrap price differential of $0.50/lb below LME is economically favorable for the membrane cell without considering benefits from melting or reusing concentrated alloying elements.
13. Even after energy reduction developments are in place, the membrane cell is expected to produce more heat than is required to melt and purify the aluminum charged to it. This extra energy could be used to preheat or melt additional aluminum.

6.0 Recommendations

The bench-scale work on the membrane purification cell process has demonstrated technological advantages and substantial energy and investment savings against other electrolytic processes. The next scale-up step would be a 500 to 1,000 Amp self-heated cell. However, prior to scale-up, the following items should be accomplished in a bench-scale cell:

1. **Selection of an optimum electrolyte.** This work documented the advantages and disadvantages of a pure fluoride electrolyte system. It allows for longer tests, eliminates constant electrolyte additions because of its non-evaporative nature, and enhances purified product coalescence, significantly improving current efficiency. However, it appeared to dissolve the alumina-based cell components. A less aggressive electrolyte needs to be identified.
2. **Membrane candidate selection.** Investigate alternative non conductive, more mechanically robust and chemically inert membrane candidates, such as boron nitride and alumina (in chloride-based electrolytes), that may offer enhanced purification performance and cell longevity.
3. **Optimized membrane cell design.** The need to assess many changing design parameters led to the geometrical cell configuration adopted in the current work. However, both the fluid flow patterns and the mass transfer conditions at the anodic and cathodic sides have not been thoroughly studied. Their influence on the purification rate is not fully understood. In particular, effects of anode-cathode distance, Ar bubbling and membrane orientation (horizontal vs. vertical) on mass transfer conditions should be quantified and understood.
4. **Close the loop on the system mass balance.** The reasons for the metal losses documented in the project should be determined. Post experimental analysis of the electrolyte composition would show if the Al undergoes chemical change(s). In addition, chemical analysis of the gray layer of each individual run is suggested. A boron nitride lining along the inner walls of the cathode graphite chamber could prevent 1) reactions of Al with graphite, and 2) avoid mechanical attrition due to physical attachment of Al particulartes to the graphite wall.

7.0 References

[1] W. Hoopes, F. C. Frary and J. D. Edwards, U.S. Patent, 1534317 (1925)

[2] S. K. Daz, C. N. Cochran, R. A. Milito, R. M. Mazgaj and W. W. Hill, U.S. Patent 4115215 (1978)

[3] K. J. Martchek, Alcoa Internal Report No. 6-81-33, 1981 July 29

[4] K. J. Martchek, Alcoa Internal Letter Report, 1981 April 28

[5] S. K. Daz and R. M. Mazgaj, Alcoa Internal Report No. 7-77-2, 1977 February 14

[6] R. A. Carpio, A. A. Fannin, Jr., F. C. Kibler, L. A. King and H. A. Oye, J. Chem. Eng. Data, 28 (1983) 34-36

[7] S. C. Jacobs, N. Jarrett, R. W. Graham, P. A. Foster, W. C. Sleppy, C. N. Cochran, W. E. Haupin and R. J. Campbell, U.S. Patent, 3852173 (1974)

[8] T. A. Utigard, R. R. Roy and K. Friesen, Can. Metall. Quart., 40 (2001) 327-334

[9] K. A. Bowman, Alcoa Internal Report No. 7-79-31, 1979 August 06

[10] P. P. Fedotieff and K. Timofeeff, Z. anorg. u. allgem. Chem., 206 (1932) 266

[11] K. Matiasovsky and M. Malinovsky, Collection Czeckoslov. Chem. Comm., 36 (1971) 3746-3751

[12] A. Dedyukhin, A. Apisarov, O. Tkacheva, A. Redkin, Yu. Zaikov, A. Frolov and A. Gusev, ECS Trans., 16 (49) 317-324

[13] E. Robert, J. E. Olsen, V. Danek, E. Tixbon, T. Ostvold and B. Gilbert, J. Phys. Chem. B, 101 (1997) 9447-9457

[14] E. Skybakmoen, A. Solheim, and A. Sterten, Metall. Mater. Trans. B, 28B (1997) 81-86

[15] R. Cassidy and J. J. Brown, J. Am. Cera. Soc., 62 (1979) 547-551

[16] V. Danek, O.T. Gustavsen and T. Ostvold, Can. Metall. Quart., 39 (2000) 153-162.

[17] J.D. Bryant and J.T. Wiswall, Economics of Aluminum Purification: R214 Processing and R1000 Processing, Alcoa Internal Report No. 11-012

8.0 Acknowledgements

The authors acknowledge the financial support from the Department of Energy - Grand Challenge Award, Contract number of DE-EE0003466. The purification cell was designed, constructed and operated by G. W. Artman, R. M. Dunlap and V. A. Paola. Coordinating work through D. D. León and S. R. Yount, and stimulating discussions with M. J. Bruno, J. D. Bryant, R. K. Dawless and E. M. Williams, are fully appreciated. The authors thank all of the contributors for their great efforts, without which the project and the report would not have been completed.